

The relevance of extensional rheology on electrospinning: the polyamide/iron chloride case

Susanna Formenti¹, Rossella Castagna¹, Roberto Momentè¹, Chiara Bertarelli¹, Francesco Briatico-Vangosa^{1*}

¹Dipartimento di Chimica Materiali e Ingegneria Chimica “G. Natta”, Politecnico di Milano, piazza Leonardo da Vinci 32, 20133 Milano, Italy

* Corresponding author. Tel.: +390223993290; email: francesco.briatico@polimi.it

Abstract

The outcomes of the electrospinning of polyamide 6 (PA6) solutions in formic acid containing FeCl₃ are correlated with the extensional rheological behaviour of these fluids, which is investigated by the self-controlled capillary breakup of a filament. The rheological analysis enlightens a significant effect of the FeCl₃ content on the rheological behaviour, the viscous component becoming predominant over a certain salt content threshold. At this concentration, the electrospun fibres show the formation of severely inhomogeneous structures this indicating that an elastically dominated behaviour is necessary to yield defect-free fibres. Addition of FeCl₃ also decreases fibre crystallinity and fibres turn out to be completely amorphous above a critical concentration. Interestingly, this concentration coincides with the one at which the viscous component starts dominating the rheological behaviour.

Keywords

Electrospinning; Capillary Breakup Extensional Rheometry; CaBER; PA6-FeCl₃ solution.

Article title: The relevance of extensional rheology on electrospinning: the polyamide/iron chloride case Article reference: EPJ7165 Journal title: European Polymer Journal Corresponding author: Dr. Francesco Briatico-Vangosa First author: Dr. Susanna Formenti Final version published online: 14-DEC-2015 Full bibliographic details: European Polymer Journal (2016), pp. 46-55 DOI information: 10.1016/j.eurpolymj.2015.12.003 © 2015. This manuscript version is made available under the CC-BY-NC-ND 4.0 license <http://creativecommons.org/licenses/by-nc-nd/4.0/>

Introduction

Conducting polymer nanofibres have gained great interest for several applications, ranging from electronics to chemical sensing, and promising developments are being widely suggested in the literature [1, 2, 3]. Currently, electrospinning is the only technique that allows the fabrication of continuous polymer nanofibres (i.e. strands with a diameter lower than 1 μm) with complex architectures [4, 5]. Although this technique is rather easy to implement for most of synthetic polymers, the processing of conducting polymers is not straightforward, due to the relatively low solubility and the limited number of entanglements of these materials. A method to overcome this issue consists in the production of a polymer mat to act as template, where an *in situ* polymerization of monomers may occur [6, 7]. This strategy has been exploited by Granato and co-workers [6] to obtain nanofibres with an insulating core and a conducting shell starting from a polyamide 6 (PA6) solution containing iron(III) chloride (FeCl_3), which promotes the following polymerization of pyrrole vapours onto the fibre surface.

Besides polymer processability, the major issue of the electrospinning technology concerns the control over the fibres morphology, as size and uniformity may significantly affect their performance [8]. A wide set of material and processing parameters can be varied to impart stability to the process, e.g. solution surface tension and electrical conductivity, applied voltage, flow rate or concentration of the polymer solution [9]. However, as in most cases complex fluids are used, the literature suggests that the formation of non-uniform electrospun structures is mainly related to rheological aspects, which are often described in terms of heuristic concepts like ‘spinnability’ and ‘stringiness’ [10, 11]. Indeed, electrospinning involves the formation, elongation and possible breakup of a liquid filament. All these phenomena occur in a free-surface elongational flow, during which the relative balance

between capillary forces and fluid viscoelasticity of the polymer solution determines the extent of local capillary thinning and of homogeneous stress, thus leading to the different types of complex morphologies. Therefore, a rigorous approach can be considered which takes into account the degree of solution elasticity of the polymer solutions [12]. As spinning technologies mainly involve extensional rather than shear deformations [12], besides the traditional shear rheometry, extensional rheometry is a valuable technique to get reliable qualitative and quantitative information on fluid viscoelasticity in free surface elongational flows [10, 13]. At present, the Capillary Breakup Extensional Rheometer (CaBER) is an accurate commercially available instrument to carry out reliable measures of viscoelastic properties of solutions.

In this context, the present work exploits the phenomenon of viscoelasto-capillary thinning in order to investigate the rheological behaviour of electrospinning solutions of PA6 and iron(III) chloride (FeCl_3) in formic acid and identify those parameters that allow the prediction of electrospun fibres morphology. This case study has been chosen as FeCl_3 is an oxidizing agent which is widely known to promote polymerization of many aromatic rings and heterocycles (e.g. pyrrole, thiophene, aniline) to afford semiconducting and conducting polymers [14]. Such kind of oxidative polymerization of the aromatic monomers has been also demonstrated to occur *in situ* onto polymer films [15, 16] and onto electrospun wire-shaped templates containing this oxidizing salt [6, 17]. However, when polyamide is used as template, the effect of FeCl_3 on the rheological properties of the polymer solution cannot be neglected, since the presence of the metal halide is known to strongly perturb or even prevent H-bonds formation between amide groups of polyamide backbones [18, 19]. Further, the system is more complex than those adopted in the literature as references due to the simultaneous occurrence of a non-diluted regime of a low molecular weight polymer in a low viscosity solvent and the presence of a third component. Hence, it may constitute a challenging benchmark for theories developed for model fluids.

Article title: The relevance of extensional rheology on electrospinning: the polyamide/iron chloride case
Article reference: EPJ7165 Journal title: European Polymer Journal Corresponding author: Dr. Francesco Briatico-Vangosa
First author: Dr. Susanna Formenti Final version published online: 14-DEC-2015 Full bibliographic details: European Polymer Journal (2016), pp. 46-55 DOI information: 10.1016/j.eurpolymj.2015.12.003 © 2015. This manuscript version is made available under the CC-BY-NC-ND 4.0 license <http://creativecommons.org/licenses/by-nc-nd/4.0/>

We demonstrate that the FeCl_3 concentration controls the rheological behaviour of the solution, which in turn influences the fibre morphology.

Experimental

Polymer Solutions

PA6 in pellets ($M_w = 10000$ g/mol), formic acid (puriss. p.a., ~98%, $\eta_s = 1.70$ mPa·s, $k = 2$ mS/cm [20]) and iron(III) hexahydrate ($\text{FeCl}_3 \cdot 6\text{H}_2\text{O}$) were purchased from Sigma Aldrich. All reagents were used as received. PA6 (15 wt% with respect to formic acid) was dissolved in formic acid under magnetic stirring at room temperature. Then, iron(III) chloride hexahydrate was added at FeCl_3 concentrations ranging between 0 and 6.5 wt% with respect to formic acid, corresponding to stoichiometric amount ranging between 0 and 28.6 mol% with respect to amide functionalities. The solution was magnetically stirred until a homogeneous phase was obtained. Hydrate salt was preferred to anhydrous FeCl_3 as the latter is highly hygroscopic thus making handling and weighting not straightforward and solution moisture-sensitive. Freshly prepared solutions were used for electrospinning and CaBER measurements.

The critical overlap concentration c^* was evaluated according to the definition provided by Graessley [21] $c^* = 0.77/[\eta]$, where $[\eta]$ is the intrinsic viscosity of the polymer solution, which is related to the polymer molecular weight M_w via the Mark–Houwink–Sakurada equation $[\eta] = K_\eta M_w^a$, where K is a constant and a depends on the solvent quality. Considering a solution containing only PA6 and formic acid, $K = 22.6 \cdot 10^{-3}$ ml/g and $a = 0.82$ [22], and thus $c^* = 1.46\%$. In the studied system, the polymer concentration is far above c^* and even about the critical entanglement concentration c_e , which is typically found to be ten times above c^* . This implies that, despite the low M_w and solvent

viscosity, the solution of 15 wt% PA6 in formic acid is expected to lead to successful fibre electrospinning [23].

Solution Characterization

Capillary Breakup Extensional Rheometry

Capillary Breakup Extensional Rheometry was adopted to investigate the extensional rheological properties of the solutions, by means of a commercially available HAAKE CaBER 1 (Thermo Fisher Scientific). In this device, a fluid is subjected to elasto-capillary self-thinning caused by an imposed step stretch deformation and the evolution of the filament diameter is monitored as the slender thread undergoes necking and finally breaks [24]. This is pursued by placing a nearly cylindrical fluid sample between two cylindrical endplates (Figure 1a), which are then rapidly separated by an imposed axial step-strain. On stretching, an elongated hourglass shaped liquid bridge forms between the plates; once the stretching has stopped, the capillary pressure causes a progressive thinning of the filament, in which a uniaxial extensional flow is produced (Figure 1b). If the liquid thread reaches the breakup, two separated drops are left on the plates (Figure 1c). During the test, the evolution of the thread midpoint diameter ($D_{mid}(t)$) is monitored by a near infra-red LASER diode assembly (Omron ZLA-4), allowing for observations about the overall extensional behaviour of the fluids as well as to extract rheological properties, if an appropriate constitutive equation is chosen to describe the fluid behaviour.

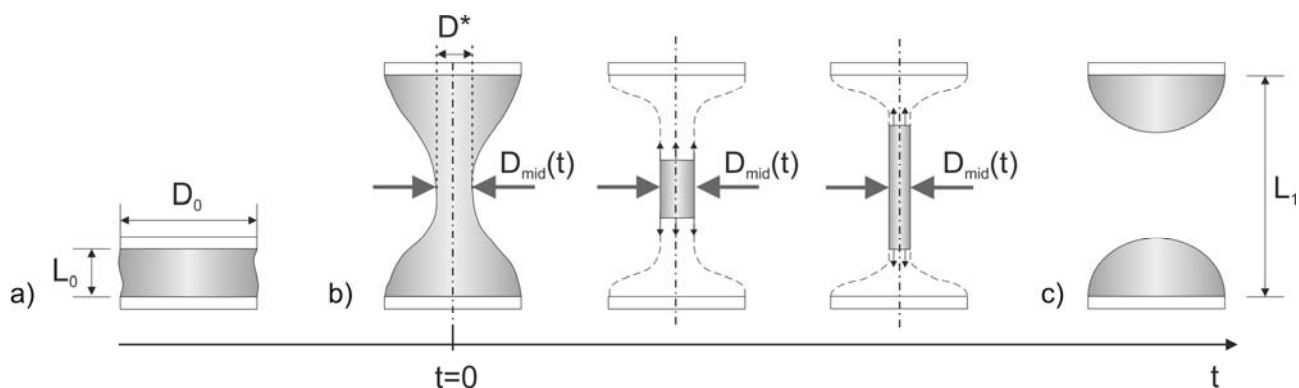


Figure 1 Operation scheme of a liquid filament rheometer and subsequent visco-elasto-capillary drainage of the fluid column: (a) initial configuration of liquid column; (b) imposed stretching deformation and liquid bridge formation; (c) eventual column breakup

In this study, the temperature of the sample chamber was controlled by a cryostat (Thermo Scientific HAAKE DC10-K10) and it was set at 25°C. The test conditions adopted to characterize all the solutions are listed in Table 1.

Table 1 Test conditions adopted for the solution characterization

Plate diameter, D_0	Sample Initial height, L_0	Sample Final height, L_1	Applied nominal Hencky strain, $\hat{\epsilon}_H = \ln L_1/L_0$	Plate separation profile
6 mm	1 mm	6 mm	1.77	Cushioned (30 ms strike time)

In addition to the laser micrometre measurements, all the tests were video-recorded with a custom-built high-speed camera system at 500 fps frame rate (frame size: 1000x1000 pixel), equipped with Computar Macro 10X lens. For the data analysis, the CaBER output, i.e. the evolution of the midpoint diameter as measured by the laser micrometre, was complemented with information from the images taken by the high-speed camera. The filament diameter after the plate separation ($D^* = D_{mid}(t=0)$) was evaluated from the video images.

The diameter evolution in time was interpreted on the basis of the analysis proposed by Entov and Hinch [25]. According to them, when a viscoelastic liquid is subjected to capillary thinning at a certain

stage the elastic stress becomes dominant and the strain rate drops, leading to a slowdown of the thinning process. The dynamics to which the filament diameter evolves is described as (Eq.1):

$$D_{mid}(t) = D^* \left(\frac{D^* G}{4\sigma} \right)^{1/3} \exp\left(-\frac{t}{3\lambda_c} \right) \quad (1)$$

where σ is the surface tension, G a shear elastic modulus, λ_c the characteristic relaxation time.

Other Characterizations

Measures of surface tension, density and shear viscosity were performed on the 0, 1, 4.5, 5.6 and 6.5 wt% solutions. Surface tension measurements were carried out with a video-based optical contact angle measuring system (DataPhysics OCA 15EC) through the pendant drop method [26]. Density was evaluated by weighting a known volume of solution (2 cm³) with an analytical balance (Mettler AE163). Shear viscosity measurements were performed with a rotational rheometer (Rheometrics DRS 200). A plate-plate geometry was used and the gap was varied between 0.5-0.7 mm. As the iron (III) chloride hexahydrate solutions are corrosive, disposable 40 mm aluminium plates were used. Scans were carried out at 30°C, imposing a linear stress ramp from 0 to 500 Pa in 3 minutes.

Electrospinning

The electrospinning process was performed at room temperature, using a bottom-up vertical configuration. The feeding solution was loaded in a 2.5 ml syringe with a 22 gauge needle (Hamilton Gaslight model 1002 TLL), mounted on an infusion pump (KDS Scientific, model series 200) which fed the polymer solution into the capillary nozzle at a constant flow rate, set at 0.05 ml/h. A high voltage power supply (Spellman SL30 P300) was connected to the needle to provide the driving voltage of 15kV. The tip-collector distance was adjusted at 20 cm and fibres were collected randomly both on glass and silicon substrates.

Article title: The relevance of extensional rheology on electrospinning: the polyamide/iron chloride case Article reference: EPJ7165 Journal title: European Polymer Journal Corresponding author: Dr. Francesco Briatico-Vangosa First author: Dr. Susanna Formenti Final version published online: 14-DEC-2015 Full bibliographic details: European Polymer Journal (2016), pp. 46-55 DOI information: 10.1016/j.eurpolymj.2015.12.003 © 2015. This manuscript version is made available under the CC-BY-NC-ND 4.0 license <http://creativecommons.org/licenses/by-nc-nd/4.0/>

Fibres Characterization

Morphological analysis of the electrospun fibres was performed on electron micrographs collected with a high resolution Scanning Electron Microscope (SEM) (FEG LEO 1525). Silicon was used as substrate and no conductive coating was applied to the samples. The diameter distribution and the mean diameter size were determined from the SEM images using the ImageJ processing software (Rasband, W.S., ImageJ, U. S. National Institutes of Health, Bethesda, Maryland, USA).

Differential Scanning Calorimetry (DSC) was employed to investigate the crystallinity of the fibres. The thermal scan was performed with a Mettler DSC-30 connected to a Mettler Toledo TC15 TA controller. All the samples underwent a thermal history constituted by i) a heating ramp from 25°C to 100°C at a 5°C/min rate to remove water from the PA fibre, ii) a cooling ramp from 100°C to 25°C at 5°C/min, iii) a two-minute isothermal step at 25°C and iv) a second heating ramp from 25°C to 250°C at 5°C/min. Data from this latter ramp were considered to estimate the degree of crystallinity in the samples. For each scan, a 50 ml/min nitrogen flux was set through the DSC camera.

Results and Discussion

Solution Characterization

All the prepared solutions were characterized by Capillary Break up Extensional Rheometry (CaBER). From the very rough outcome it appears that the measures have been performed close to the limit of the instrument resolution, as the fluids were characterized by a very fast diameter evolution if compared to simpler model liquids [27, 10]. Nevertheless, the measurements were satisfactorily repeatable as reported in SI.

Figure 2 shows the differences in the thinning dynamics for solutions with different salt content. It can be observed that the shape of the diameter evolution curves progressively moves towards purely viscous-like one [24] as the content of FeCl₃ exceeds the 5 wt%. This is clearer if the diameter axis is reported in a logarithmic scale (Figure 2b).

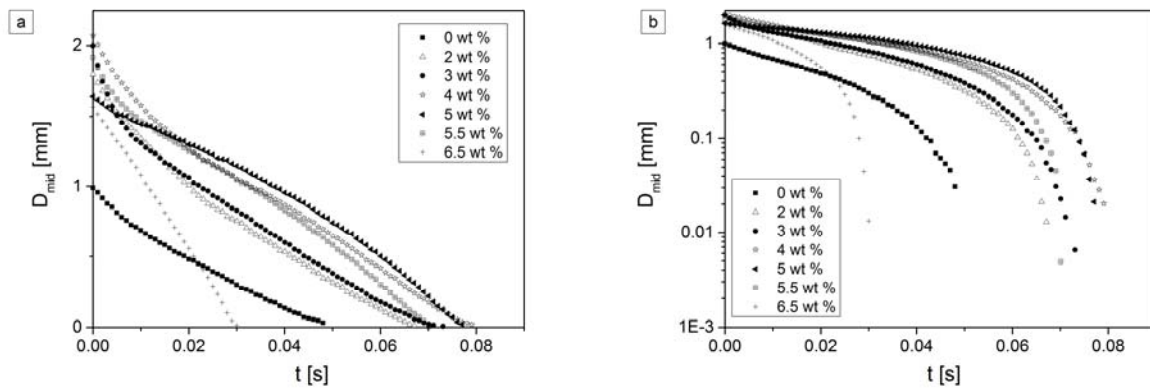


Figure 2 Evolution of mid filament diameter as function of time for the PA6 in formic acid solutions (15 wt%, Mw ~10 kg/mol) for different FeCl₃ content, expressed as weight percentage with respect to formic acid. For the sake of clarity, only some concentrations are reported. a) Mid filament diameter represented in a linear scale; b) Mid filament diameter represented in a logarithmic scale.

In order to select the time range in which the breakup phenomenon is ruled by the elasto-capillary balance, the approach proposed by Clasen for the case of semi-diluted solution [28] was adopted. The

extension rate, $\dot{\epsilon} = -\frac{2}{D_{mid}} \frac{dD_{mid}}{dt}$, was calculated from experimental data, as reported in Figure 3 for

the 3 wt% FeCl₃ solution. Equation 1 was then applied to the final part of the $D_{mid} - t$ curve, where $\dot{\epsilon}$ reaches a constant value. This procedure was applied to all solutions except for the 6.5 wt% one, as in this case no constant value can be observed for $\dot{\epsilon}$, probably due to the limited resolution of the CaBER micrometre.

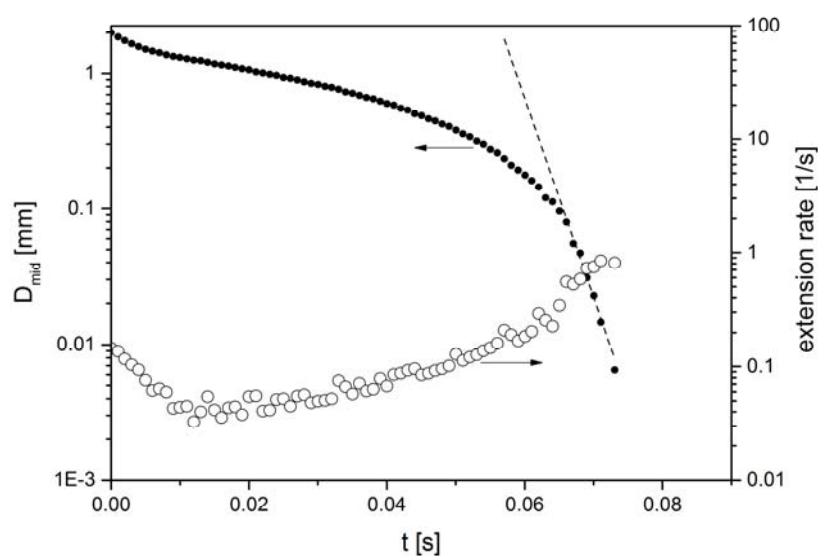


Figure 3 Evolution of mid filament diameter and extension rate as a function of time for the PA6 in formic acid solutions (15 wt%, Mw ~10 kg/mol) containing 3 wt% of FeCl₃ with respect to solvent. The dashed line represents the fitting according to Equation 1.

The effect of iron chloride concentration on the characteristic time of viscoelastic relaxation, λ_C , is reported in Figure 4. λ_C is found to be almost constant until 3.5 wt%, then a slight increase occurs at intermediate concentrations and finally it drops to low values at 5.6 wt%.

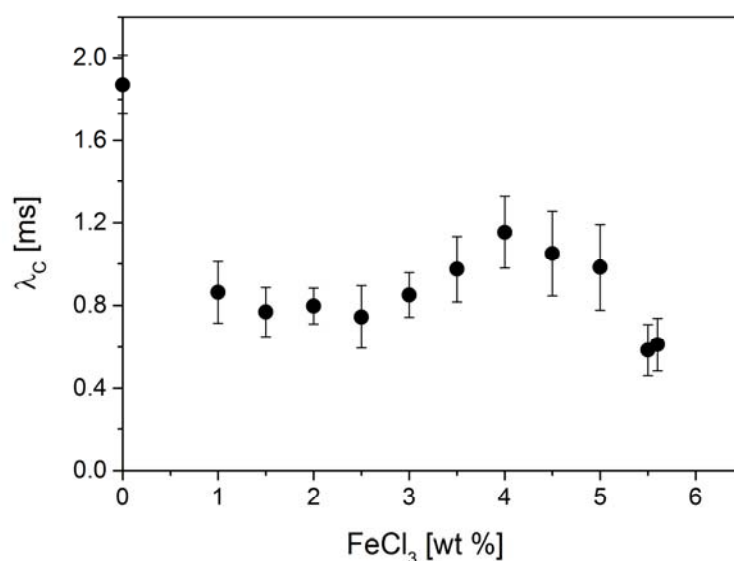


Figure 4 Polymer relaxation time as a function of the FeCl₃ content (weight percentage with respect to solvent) in solutions of PA6 (15 wt%, Mw ~10 kg/mol) and formic acid.

Both the drop in λ_c when FeCl₃ is added to the PA6 solution and its decrease at the highest salt concentrations are consistent with the scission of the H-bond between amide groups, which reduces the solution elasticity and, as a consequence, the relaxation time. The trend at intermediate salt content cannot be explained with the same phenomenon. In any case, in light of the presented results, the presence of the iron chloride is supposed to induce different transitions in the solution behaviour.

Table 2 shows negligible effect of salt content on density and surface tension, which can be then considered constant, with a mean value of 1.23 ± 0.01 g/cm³ and 39.51 ± 0.13 mN/m, respectively. Considering the latter, PA6 slightly increases the surface tension of the solution, with respect to that of the solvent alone ($\sigma_{solvent}=37.84$ mN/m). Interestingly, the mean value is quite low with respect to other polymeric solutions [12]. As surface tension acts as driving force in capillary instabilities, the low σ value would limit the onset of jet instabilities and beads formation during the electrospinning process.

Table 2 Properties of the PA6 (15 wt%) in formic acid solutions for different FeCl₃ content: density, surface tension and zero shear viscosity

wt% FeCl ₃	mol% FeCl ₃	ρ [g/cm ³]	σ [mN/m]	η_0 [Pa.s]
0	0	1.230	39.6 ± 0.2	0.217
1	4.5	1.231	39.4 ± 0.1	0.312
4.5	19.6	1.224	39.6 ± 0.2	0.379
5.6	24.7	1.228	39.6 ± 0.2	0.438
6.5	28.6	1.255	39.3 ± 0.2	0.490

The measured shear viscosity versus shear rate for the five tested solutions is shown in Figure 5. Shear rates were limited to 10² s⁻¹ during the tests to avoid problems related to humidity uptake and chemical reactions between the solutions and aluminium plates. Of course, the shear rate range is limited with respect to the deformation rates applied to the solutions during electrospinning. Thus, as these values have to be considered with caution, only the zero shear viscosity was considered, accordingly.

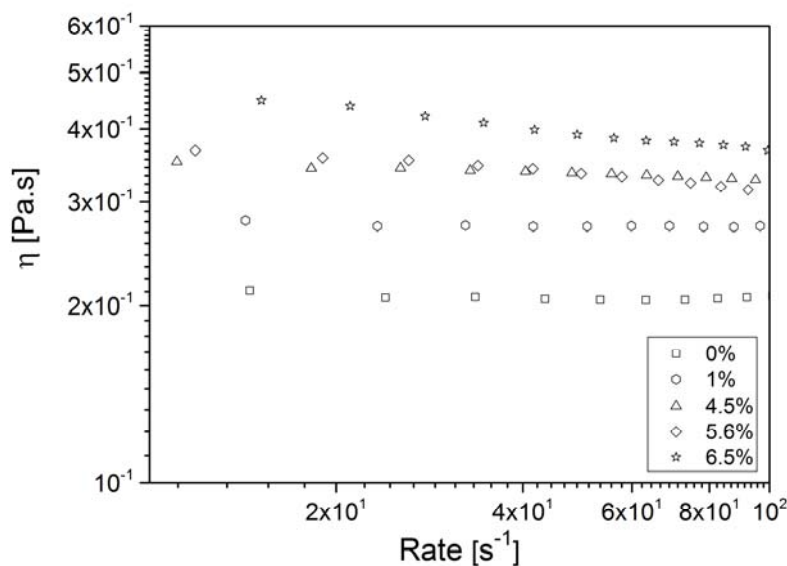


Figure 5 Viscosity measurement as a function of shear rate for different content of FeCl₃ in 15 wt% PA6 solution in formic acid.

At low FeCl₃ contents, the solutions behave like Newtonian fluids, with shear viscosities being independent on the shear rate in the investigated range. On the other hand, at high FeCl₃ contents, the

shear behaviour appears to be slightly shear thinning. Nevertheless, if the analysis is limited to this limited shear rate range, in which the flow curve is unaffected by solution alterations, it is possible to observe that the higher the content of FeCl_3 , the higher the shear viscosity (Figure 5). This result can be explained assuming that the macromolecular coils are swollen because of the steric hindrance of the hexahydrate chloride molecules. Under shear, this effect is similar to the one caused by raising the polymer molecular weight, that is a viscosity increase due to the enhancement of coil interactions. This observation appears in contrast with the results of extensional measures; however, shear and elongation imply different mechanism of chain deformation. The effect of steric hindrance may not be predominant in the case of elongational flow, in which the most relevant effect of the salt seems to be the reduction of chain interactions through H-bond scission, rather than chain solvation.

Electrospun Fibre Characterization

As a general remark, all the fibrous membranes show an almost uniform morphology, until 6.5 wt% (28.7 mol%) content is reached (Figure 6): at this critical concentration, only beaded fibres are collected. Also, branching effectively occurred in electrospinning pure PA6 solution, which is typical of excess charge accumulation.

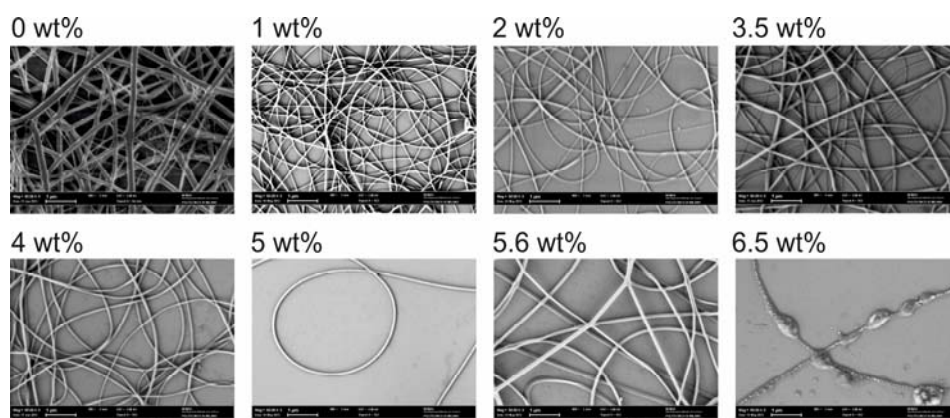


Figure 6 SEM images of electrospun fibres mats obtained from feed solutions of formic acid and 15 wt% of PA6 (Mw ~10 kg/mol) with different FeCl₃ content.

The analysis of the fibre diameter distribution showed a Gaussian statistic for about all the solutions, with the exception of the branched fibres, for which a bimodal distribution is observed. In these instances the mean diameter size reported, \bar{d} does not consider the branched fibres. It was also observed that for higher content of the ionic salt more homogeneous fibres were obtained, as reported in the work of Cai and co-workers [29].

As it can be observed in Figure 7, the fibre diameter reduces by more than four times when adding the 1 wt% (4.5 mol%) of FeCl₃ with respect to the PA6 solution without salt. For FeCl₃ concentrations above 1 wt%, \bar{d} increases progressively up to 5.6 wt% (24.7 mol%).

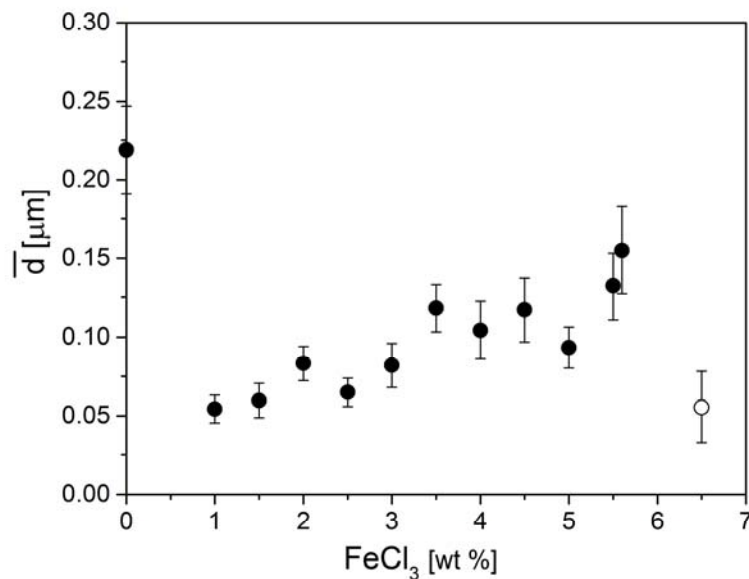


Figure 7 Mean diameter size as function of FeCl₃ content (weight percentage with respect to solvent) in solutions of 15 wt% PA6 (Mw ~10 kg/mol) and formic acid. The diameter size of the fibre obtained by electrospinning the 6.5 wt% FeCl₃ solution is represented with a hollow symbol to underline that in this case \bar{d} is just a rough estimation due to the presence of several non-homogeneities.

A clear interpretation of the trend shown in Figure 7 is actually not straightforward; indeed, the literature provides many attempts of prediction of the final electrospun fibre diameters considering a single material property, such as the zero shear viscosity of the feed solution. Anyway, these empirical approaches are often appropriate only for specific polymer-solvent combinations [13].

For example, in the present study, the presence of the ionic salt in solution should not be overlooked *a priori*, as the addition of charged species may change the solution conductivity [29, 30, 31] and influence the onset and growth of the bending and capillary instabilities and the final fibre diameter [32]. To verify this hypothesis, the electrical conductivity of the system was measured for four different salt concentrations (0, 1, 4 and 5.5 wt%). The results revealed that the solution has a mean conductivity of 4.30 ± 0.09 mS/cm, regardless of FeCl₃ content, and therefore the change in the fibre diameter cannot be likely ascribed to this parameter. Further, literature usually reports an enhancement in the jet stability through the increase in conductivity produced by the added ionic species [13, 32, 33]: in the present case, a transition from stable to unstable jet is observed when 6.5 wt% (28.7 mol%) FeCl₃ is added to the PA6 solution.

A different interpretation of these results may be sought in the rheological behaviour. At intermediate salt contents, some correlation can be observed between the increase in zero shear viscosity (Figure 5), due to chain solvation at increasing salt content, and the progressive increase of the fibre diameter (Figure 7). Anyhow, these considerations are roughly qualitative, as the zero shear viscosity is not the proper material property to be considered for this correlation. The work by Helgeson and co-workers [13] points out that, in the case of strong extensional flow, such as in the electrospinning process, the finite extensibility viscosity limit stabilizes the solution jet, thus playing a dominant role in determining the fibre morphology and diameter. At present no rheological methods allows for a reliable evaluation of extensional viscosities at these extension rates [13]. In this work, during the

CaBER experiments the solutions were subjected to a maximum extension rate that was at least two orders of magnitude less than the typical one experienced during the electrospinning process.

Considering the solution elasticity, it is worth noting that the trend of the polymer relaxation time (Figure 4) is in nice agreement to the one of fibre diameter size in Figure 7. Indeed, the addition of 1 wt% (4.5 mol%) of FeCl₃ to the pure PA6 and formic acid solution causes a drop both in λ_c and \bar{d} . This is even more evident if the transition between the 5.6 and 6.5 wt% (24.7 and 28.7 mol%) solutions is considered: the lack of an identifiable elasto-capillary balance concurs with the production of severely ill-formed fibres.

Another interesting observation, which enlightens again the presence of strong interactions between PA6 and FeCl₃, concerns the morphology of the fibres electrospun from the 6.5 wt% (28.7 mol%) solution. The polymer concentration in the studied system is around c_e and thus it is above the concentration set as minimum value for the solution to be spun [23]. Nevertheless, when a critical threshold of salt content exceeds, a good spinnability condition cannot be achieved anymore, despite the polymer concentration should be in principle high enough. This is not normally observed in literature where the jet stability is enhanced through the increase in conductivity produced by the added charged species [13, 32, 33].

A direct effect of FeCl₃ on the rheological behaviour of the studied solutions is therefore observable, and it seems to affect also the electrospinning outcomes. According to Helgeson and co-workers [13] the stress stabilizing the jet during electrospinning is determined by the finite extensibility viscosity limit. Even if no direct measurement of this property is available, the limited change in viscosity and relaxation times suggest only small change in the finite extensibility. This indicates that an explanation of the observed change in diameter with FeCl₃ cannot be given in term of its effects on

the solution rheology alone. As the stabilizing stress is the product of the finite extensibility viscosity by the elongation rate, an effect of the salt on extension rate cannot be excluded.

Thermal analysis (Figure 8a) reveals a melting peak in thermograms up to 4.5 wt% (19.6 mol%) FeCl_3 , meaning that higher salt concentrations leads to amorphous fibres, as confirmed by the lack of the endothermic peak in the 5.6 wt% scan.

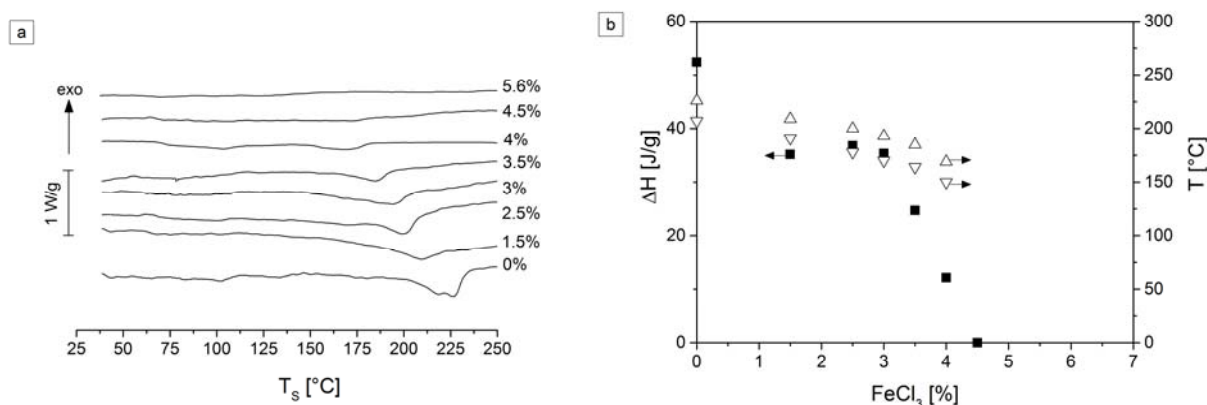


Figure 8 a) DSC thermograms of PA6 (15 wt%) in formic acid solutions with different FeCl_3 content; b) melting enthalpy (square), melting onset temperature (downward triangle) and melting temperature (upward triangle) as a function of the FeCl_3 content.

When present, the melting peak is very broad, which is a sign of the scattered distribution of the crystal size. Moreover, a correlation exists between the amount of FeCl_3 in solution and the extent and position of the peaks. Quantitative validations of these observations were obtained considering the melting enthalpies (peak area) and temperatures (peak position) of the fibres showing that the higher the iron chloride content, the lower the melting enthalpies, the melting temperature and the temperature at melting onset (Figure 8b). The FeCl_3 effect on fibres crystallinity is thus apparent. An interpretation of these results can be given according to the literature that reports on the effect of inorganic salt on bulk properties of different polymers [29, 34, 35]. In the present work, these effects are ascribed to the site-specific hydrogen bonds cleavage due to the interaction between the lone pairs of the oxygen of the amide groups and the iron trichloride, which is a strong Lewis acid.

The most interesting result comes from the observed correlation between the rheological behaviour of the solutions and the crystallinity of the electrospun fibres. Indeed, fibres become completely amorphous as soon as the shear viscosity curves start displaying a slight shear thinning behaviour. Nevertheless, it seems that the crystallinity is influenced but not essentially controlled by the flow behaviour, but rather by the steric hindrance of the salt, since the same transition in similar systems was observed also in crystallization in quiescent conditions [29, 35].

Adimensional Analysis and Results Correlation

Adimensional analysis represents an effective tool to interpret the behaviour of a system in complex flows [36, 37]. In the case of electrospinning it can be successfully applied for model polymer solutions [12]. Indeed, this method allows to establish whether a solution is viscoelastic or not, but also to effectively relate the rheological behaviour to the heuristic and poorly quantified concept of ‘spinnability’. Following McKinley’s approach [37], three adimensional quantities were evaluated for some solutions of this study: the intrinsic Deborah number ($De_0 = \lambda / \sqrt{\rho D^3 / \sigma}$), describing whether elastic stresses are large enough to dominate on capillarity, the Ohnesorge number ($Oh = \eta_0 / \sqrt{\rho \sigma D}$), that estimates the relative importance of the viscous stresses with respect to capillary action, and the Elastocapillary number ($Ec = De_0 / Oh = \lambda_c \sigma / \eta_0 D$), which represents the relative magnitude of elastic stresses with respect to viscous ones. Based on Clasen and co-workers [28, 36], the average mid-filament diameter measured when the breakup phenomenon is ruled by the elasto-capillary balance was adopted to determine the “local” adimensional numbers.

Table 3 Local adimensional numbers evaluated for four different FeCl₃ content in PA6 (15 wt%) and formic acid solutions

wt% FeCl ₃	mol% FeCl ₃	<i>Oh</i>	<i>De₀</i>	<i>Ec</i>
0	0	3.09	10.33	3.34
1	4.5	3.84	3.06	0.79

4.5	19.6	4.08	2.49	0.61
5.6	24.7	6.76	4.28	0.63

Table 3 reports the effect of FeCl₃ content on the local adimensional numbers. It can be observed that De_0 is always higher than 1, as expected, indicating the viscoelastic behaviour of the solutions. However, for all the solutions containing FeCl₃ $De_0 < 6$, the value indicated in [12] as threshold for the formation of stable electrospun fibres. Further, for all the considered solutions $Ec < 4.71$ and therefore the breakup phenomenon seems to be viscously dominated [36] in all the considered case. Thus, the analysis based on adimensional numbers fails in correctly predicting the spinnability of the present solutions, probably because the characteristic time of the studied system is similar or even a little shorter than the timescales typical of filament breakup, which in turn are significantly longer than those typical of the electrospinning process.

Conclusions

In this work, the outcomes of the electrospinning of polyamide 6 (PA6) in formic acid containing FeCl₃ are correlated with the rheological behaviour of the feed solutions, investigated through the phenomenon of self-controlled capillary breakup of a filament. The rheological analysis enlightens a significant effect of the FeCl₃ content on the rheological behaviour. The addition of the ionic salt to the PA6 solutions lowers solution elasticity due to the hydrogen bond scission, induced by the formation of complexes between the salt and the amide groups of the PA6 backbones. Simultaneously, it increases the shear viscosity, likely due to the swelling of the macromolecular coils because of the steric hindrance of FeCl₃, coordinated to the polymer backbone. At 6.5 wt% (28.7 mol%) concentration the elasto-capillary balance is no more observed to rule the breakup

phenomenon, and a relaxation time cannot be determined. The morphological observations on the

Article title: The relevance of extensional rheology on electrospinning: the polyamide/iron chloride case
 Article reference: EPJ7165 Journal title: European Polymer Journal Corresponding author: Dr. Francesco Briatico-Vangosa
 First author: Dr. Susanna Formenti Final version published online: 14-DEC-2015 Full bibliographic details: European Polymer Journal (2016), pp. 46-55 DOI information: 10.1016/j.eurpolymj.2015.12.003 © 2015. This manuscript version is made available under the CC-BY-NC-ND 4.0 license <http://creativecommons.org/licenses/by-nc-nd/4.0/>

same solution show a significant formation of defects in the collected fibres, even if the concentration of PA6 in formic acid is around the critical entanglement concentration.

As the increase in salt content does not influence the conductivity of the PA6 solution, its effects on the final fibres morphology is at least partly related to the change induced by FeCl₃ in the rheological behaviour of the considered system. Other effects related to the flow condition during the electrospinning cannot nevertheless be excluded.

Besides the aforementioned effects, FeCl₃ was shown to affect the electrospun fibre crystallinity, as above a critical concentration fibres turn out to be completely amorphous. Interestingly, this concentration coincides with that one at which the viscous components starts playing a significant role in the rheological behaviour, which is about 4 wt% FeCl₃ content. Steric hindrance of FeCl₃ is likely the origin of both observations, which occur independently one with respect to the other.

To conclude, we demonstrated that the additivition of the electrospinning feed solution has a relevant effect and should be carefully controlled in order to ensure that the process is dominated by fluid elasticity. Elastically stabilized solutions are required to produce defect-free fibres.

Author Contributions

The manuscript was written through contributions of all authors. All authors have given approval to the final version of the manuscript.

References

Article title: The relevance of extensional rheology on electrospinning: the polyamide/iron chloride case Article reference: EPJ7165 Journal title: European Polymer Journal Corresponding author: Dr. Francesco Briatico-Vangosa First author: Dr. Susanna Formenti Final version published online: 14-DEC-2015 Full bibliographic details: European Polymer Journal (2016), pp. 46-55 DOI information: 10.1016/j.eurpolymj.2015.12.003 © 2015. This manuscript version is made available under the CC-BY-NC-ND 4.0 license <http://creativecommons.org/licenses/by-nc-nd/4.0/>

- [1] H. Bagheri and A. Aghakhani, "Polyaniline-Nylon-6 Electrospun Nanofibers for Headspace Adsorptive Microextraction," *Anal. Chim. Acta*, no. 713, p. 63–69, 2012.
- [2] H. Dong, U. Megalamane and W. Jones, "Conductive polyaniline/PMMA Coaxial Nanofibers: Fabrication and Chemical Sensing," *Abstracts of Papers of the American Chemical Society*, no. 226, p. 1155, 2003.
- [3] X. Wang, C. Drew, S. Lee, K. J. Senecal, J. Kumar and L. Samuelson, "Electrospun Nanofibrous Membranes for Highly Sensitive Optical Sensors," *Nano Lett.*, no. 2, p. 1273–1275, 2002.
- [4] A. Greiner and J. H. Wendorff, "Electrospinning: A Fascinating Method for the Preparation of Ultrathin Fibers," *Angew. Chem. Int. Ed. Engl.*, no. 46, p. 5670–5703, 2007.
- [5] W. E. Teo and S. Ramakrishna, "A Review on Electrospinning Design and Nanofibre Assemblies," *Nanotechnology*, no. 17, p. R89–R106, 2006.
- [6] F. Granato, A. Bianco, C. Bertarelli and G. Zerbi, "Composite Polyamide 6/Polypyrrole Conductive Nanofibers," *Macromolecular Rapid Communications*, vol. 30, pp. 453–458, 2009.
- [7] R. Castagna, R. Momentè, G. Pariani, G. Zerbi, A. Bianco and C. Bertarelli, "Highly homogeneous core-sheath polyaniline nanofibers by polymerisation on wire-shaped template," *Polymer Chemistry*, vol. 5, pp. 6779–6788, 2014.
- [8] M. Ma, Y. Mao, M. Gupta, K. K. Gleason and G. C. Rutledge, "Superhydrophobic fabrics produced by electrospinning and chemical vapor deposition," *Macromolecules*, vol. 38, no. 23, pp. 9742–9748, 2005.

- [9] S. Ramakrishna, K. Fujihara, W. Teo, T. Lim and Z. Ma, *An Introduction to Electrospinning and Nanofibers*, World Scientific Publishing Company, 2005.
- [10] G. H. McKinley, “Visco-elasto-capillary thinning and break-up of complex fluids,” *HML report*, 2005.
- [11] W. M. Jones and L. J. Rees, “The Stringiness of Dilute Polymer Solutions,” *J.Non-Newtonian Fluid Mech.*, no. 11, pp. 257-268, 1982.
- [12] J. H. Yu, S. V. Fridrikh and G. C. Rutledge, “The role of elasticity in the formation of electrospun fibers,” *Polymer*, vol. 47, no. 13, pp. 4789-4797, 2006.
- [13] M. E. Helgeson, K. N. Grammatikos, J. M. Deitzel and N. J. Wagner, “Theory and kinematic measurements of the mechanics of stable electrospun polymer jets,” *Polymer*, vol. 49, pp. 2924-2936, 2008.
- [14] T. Skotheim and J. Reynolds, *Handbook of Conducting Polymers*, CRC Press, 2007.
- [15] Y. Park, S. Choi, S. K. Song and S. Miyata, “Synthesis of highly conducting nylon-6 composites and their electrical properties,” *Journal of Applied Polymer Science*, vol. 45, no. 5, pp. 843-851, 1992.
- [16] J. Rabek, J. Lucki, H. Kereszti, B. Krische, B. J. Qu and W. F. Shi, “Polymerization of pyrrole on polyether, polyester and polyetherester-iron (III) chloride coordination complexes,” *Synthetic Metals*, vol. 45, no. 3, pp. 335-351, 1991.
- [17] D. Chen, Y. Miao and T. Liu, “Electrically Conductive Polyaniline/Polyimide Nanofiber Membranes Prepared via a Combination of Electrospinning and Subsequent In situ Polymerization Growth,” *Applied Materials Science and Interfaces*, vol. 5, p. 1206–1212, 2013.

- [18] M. Hernandez, L. Servant, J. Grondin and J. C. Lassègues, "Spectroscopic Characterization of Metal Chloride/Polyamide Complexes," *Ionics 1*, pp. 454-468, 1995.
- [19] J. C. Lassègues, J. Grondin, M. Hernandez, L. Servant, S. J. Wen and L. Fournes, "Spectroscopic study of the complexation between nylon-6 and FeCl₃," *New J. Chem.*, vol. 20, pp. 317-329, 1996.
- [20] R. Weast, Handbook of chemistry and physics - 52th Edition, Cleveland: Chemical Rubber Publishing Company, 1971.
- [21] W. W. Graessley, "Polymer chain dimensions and the dependence of viscoelastic properties on the concentration, molecular weight and solvent power," *Polymer*, vol. 21, p. 258–262, 1980.
- [22] J. Brandrup, E. H. Immergut and W. McDowell, Polymer Handbook - 2nd edition, New York: John Wiley & Sons, 1974.
- [23] L. Palangetic, N. K. Reddy, S. Srinivasan, R. E. Cohen, G. H. McKinley and C. Clasen, "Dispersity and spinnability: Why highly polydisperse polymer solutions are desirable for electrospinning," *Polymer*, vol. 55, no. 19, p. 4920–4931, 2014.
- [24] G. H. McKinley and A. Tripathi, "How to Extract the Newtonian Viscosity from Capillary Breakup Measurements in a Filament Rheometer," *J. Rheol.*, vol. 44, no. 3, pp. 653-670, 2000.
- [25] V. M. Entov and E. J. Hinch, "Effect of a spectrum of relaxation times on the capillary thinning of a filament of elastic liquid," *Journal of Non-Newtonian Fluid Mechanics*, vol. 72, no. 1, pp. 31-53, 1997.
- [26] A. W. Adamson and A. P. Gast, Physical chemistry of surfaces, Interscience publishers New York, 1967.

- [27] S. L. Anna and G. H. McKinley, "Elasto-capillary Thinning and Breakup of Model Elastic Liquids," *J. Rheol.*, vol. 45, no. 1, pp. 115-138, 2001.
- [28] C. Clasen, "Capillary breakup extensional rheometry of semi-dilute polymer solutions," *Korea-Australia Rheology Journal*, vol. 22, pp. 331-338, 2010.
- [29] Y. Cai, D. Gao, Q. Wei and others, "Effects of ferric chloride on structure, surface morphology and combustion property of electrospun polyacrylonitrile composite nanofibers," *Fibers and Polymers*, vol. 12, no. 1, pp. 145-150, 2011.
- [30] K. P. Matabola and R. M. Moutloali, "The influence of electrospinning parameters on the morphology and diameter of poly(vinylidene fluoride) nanofibers- effect of sodium chloride," *J Mater Sci*, no. 48, p. 5475–5482, 2013.
- [31] K. Nartetamrongsutt and G. G. Chase, "The influence of salt and solvent concentrations on electrospun polyvinylpyrrolidone fiber diameters and bead formation," *Polymer*, vol. 54, no. 8, pp. 2166-2173, 2013.
- [32] H. Fong, I. Chun and D. Reneker, "Beaded nanofibers formed during electrospinning," *Polymer*, vol. 40, no. 16, pp. 4585-4592, 1999.
- [33] K. Arayanarakul, N. Choktaweasap, D. Aht-ong, C. Meechaisue and P. Supaphol, "Effects of Poly(ethylene glycol), Inorganic Salt, Sodium Dodecyl Sulfate, and Solvent System on Electrospinning of Poly(ethylene oxide)," *Macromolecular Materials and Engineering*, vol. 291, no. 6, p. 581–591, 2006.
- [34] H. W. Starkweather Jr and P. Avakian, "Effect of adsorbed salts on the conductivity of nylon 66," *Macromolecules*, vol. 26, no. 23, pp. 6217-6219, 1993.

- [35] B. Valenti, E. Bianchi, G. Greppi, A. Tealdi and A. Ciferri, "Bulk properties of synthetic polymer-inorganic salt systems. Melting behavior of salted poly (caproamide)," *The Journal of Physical Chemistry*, vol. 77, no. 3, pp. 389-395, 1973.
- [36] C. Clasen, P. M. Phillips, L. Palangetic and J. Vermant, "Dispensing of rheologically complex fluids: the map of misery," *AIChE Journal*, vol. 58, no. 10, pp. 3242-3255, 2012.
- [37] G. H. McKinley, "Dimensionless Groups for Understanding Free Surface Flows of Complex Fluids," *Soc. Rheol. Bulletin*, vol. July, pp. 6-9, 2005a.